Interface mode between gyroelectric and hyperbolic media

D. B. Provenzano
Scuola Normale Superiore, I-56126 Pisa, Italy

G. C. la Rocca
Scuola Normale Superiore, I-56126 Pisa, Italy and
NEST - National Enterprise for nanoScience and nanoTechnology, 56127 Pisa, Italy
(Dated: December 2022)

We report the prediction of a novel type of electromagnetic surface wave which propagates at the interface between a gyroelectric material and a hyperbolic medium. By solving Maxwell's equations, the existence conditions of this surface mode are discussed as determined by the media parameters, the working frequency and the direction of the principal axes of the hyperbolic medium. As one would expect, gyrotropy gives non-reciprocal features to these waves, such as the asymmetry between the forward propagation and the backward propagation. We show that the field distribution of the new wave resembles the Zenneck wave's one, albeit in the present case material losses are not required. Finally, we analyze a realistic configuration which supports the surface modes here predicted and allows for their excitation.

I. INTRODUCTION

Electromagnetic Surface Waves (ESWs) have attracted the attention of many researchers since the work of Jonathan Zenneck in 1907 [1]. Surface modes can exist under certain conditions on a surface bounded by air, or at the interface separating two semi-infinite half-spaces [2]. ESWs propagate along the interface and decay exponentially in the normal direction. The most remarkable examples of ESWs are Surface Plasmon-Polaritons (SPPs), highly localized ESWs which propagate at the interface between two isotropic media with opposite-sign permittivities [3]. Nowadays SPPs dominate the nanotechnology scene, at least at optical frequencies, and are exploited in many applications, such as bio-sensors and near-field optics [4]. Other remarkable electromagnetic surface modes are the Zenneck Waves (ZWs). They can exist at the interface between a lossless dielectric and a lossy one and, like SPPs, have a TM nature. Their most peculiar features are the attenuation in the longitudinal direction – caused by absorption in the lossy medium – and a tilt of the field distribution with respect to the normal to the interface [5, 6].

Some remarkable cases of surface waves at the interface between an anisotropic material and an isotropic one were analyzed in detail in previous works [7–16]. In [7] Dyakonov's Waves (DWs) were shown to propagate between an isotropic dielectric and an uniaxial crystal whose optical axis lied on the interface. DWs are hybrid-polarized waves which can propagate only in a small angular range with certain orientation relative to the optical axis. If one of the media has metal-like permittivities, DWs become Dyakonov Plasmons (DPs) [9, 16]. These modes inherit the main features of SPPs and DWs, i.e. high localization and strong directionality, respectively.
If the system is placed in an external magnetic field, some kinds of media are likely to exhibit non-reciprocal behaviours which can strongly affect the propagation of ESWs [10–12]. Gyrotropy gives unique features to these modes, such as non-reciprocity in the dispersion and the lack of time-reversal symmetry. Nevertheless, few works concern the propagation of other kinds of surface modes between two anisotropic half-spaces [17–21].

In the present paper, we focus on the analysis of electromagnetic surface modes localized at the interface between a gyrotropic material and an uniaxial medium. In particular, our aim is to study the features of a novel type of ESW propagating between an electrically-gyrotropic material and a Hyperbolic Medium (HM). We show that the anisotropy of the HM is responsible for a tilted behaviour in the field lines of the mode, which resemble those of the ZW for lossy metals. Furthermore, we show that gyrotropy is responsible for the multiplicity of these modes and gives them non-reciprocal dispersion features. We finally provide the analysis of a realistic gryroelectric-hyperbolic interface - composed of InSb and a stuck of graphene layers - which could be exploited in order to detect such new modes.

II. SURFACE WAVES PROPAGATING BETWEEN TWO SEMI-INFINITE MEDIA

Let us analyze the propagation of surface waves at the interface between a gyroelectric and an uniaxial medium (possibly a HM), as outlined in Fig. 1. We chose to consider a gyroelectric medium in the so called *Voigt configuration*, such that in our coordinate system its dielectric tensor reads

$$\boldsymbol{\epsilon}_{gyro} = \epsilon_0 \begin{pmatrix} \epsilon_B & 0 & 0 \\ 0 & \epsilon_g & ig \\ 0 & -ig & \epsilon_g \end{pmatrix}, \tag{1}$$

which is equivalent to considering an external magnetic field pointing towards the x-axis. As for the uniaxial

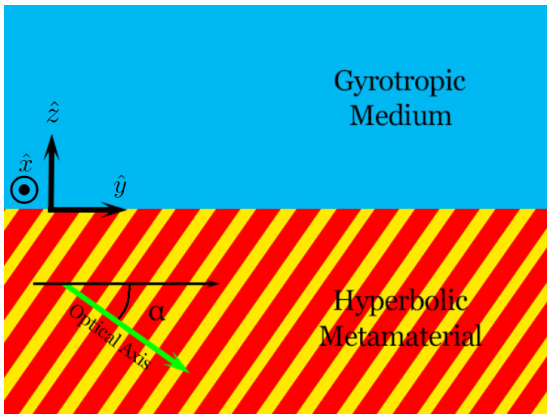

FIG. 1. Outline of the interface between a gyroelectric medium and a hyperbolic medium. The green line represents the direction of the optical axis of the hyperbolic medium.

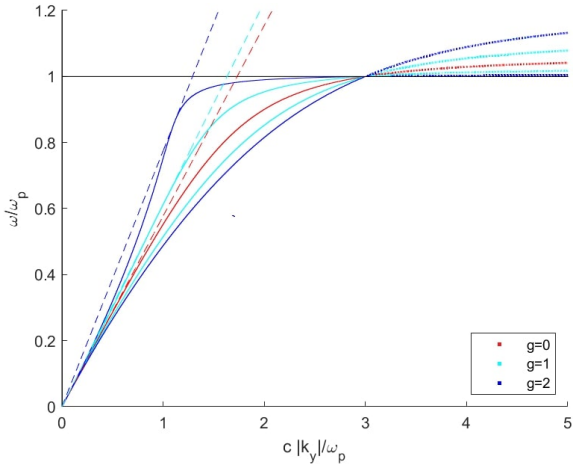

FIG. 2. Typical dispersion diagrams of a surface wave travelling through the interface between a gyroelectric medium and an HM (the parameters used for illustrative purposes are $\epsilon_g = 3$ and $\epsilon_\perp = 9$). The dashed lines represent the light dispersion in the gyroelectric medium. The multiplicity of full lines of the same colour is due to $\pm$ sign in Eq. (19) and refers to forward and backward propagating waves. In particular, each upper branch represents a forward mode, whereas each lower branch represents a backward mode. The red curve describes the case with no gyrotropy, hence its corresponding wave can propagate in both directions. It is to be noted that for $\omega > \omega_p$ all curves shown no longer correspond to physically acceptable solutions, but rather represent the real part of an in-plane wave-vector k_y which is no longer real.

medium, its dielectric tensor was chosen to be

$$\boldsymbol{\epsilon}'_u = \epsilon_0 \begin{pmatrix} \epsilon_\perp & 0 & 0 \\ 0 & \epsilon_\parallel & 0 \\ 0 & 0 & \epsilon_\perp \end{pmatrix}, \tag{2}$$

in its principal coordinate system. We consider the configuration wherein the optical axis is neither parallel nor perpendicular to the interface between the two media, as shown Fig. 1. Hence, we have to rotate the dielectric tensor by means of the rotation matrix

$$R_x(\alpha) = \begin{pmatrix} 1 & 0 & 0 \\ 0 & \cos\alpha & \sin\alpha \\ 0 & -\sin\alpha & \cos\alpha \end{pmatrix}. \tag{3}$$

In our coordinate system, the uniaxial dielectric tensor reads

$$\boldsymbol{\epsilon}_u = R_x(\alpha)\ \boldsymbol{\epsilon}'_u\ R_x(-\alpha) = \epsilon_0 \begin{pmatrix} \epsilon_{xx} & 0 & 0 \\ 0 & \epsilon_{yy} & \epsilon_{yz} \\ 0 & \epsilon_{zy} & \epsilon_{zz} \end{pmatrix}, \tag{4}$$

where the matrix elements are

$$\begin{cases} \epsilon_{xx} = \epsilon_\perp, \\ \epsilon_{yy} = \epsilon_\perp \sin^2\alpha + \epsilon_\parallel \cos^2\alpha, \\ \epsilon_{yz} = \epsilon_{zy} = \left(\epsilon_\perp - \epsilon_\parallel\right) \sin\alpha \cos\alpha, \\ \epsilon_{zz} = \epsilon_\perp \cos^2\alpha + \epsilon_\parallel \sin^2\alpha. \end{cases} \tag{5}$$

The condition for the surface wave to exist is its evanescence far from the interface, hence in both regions the wave vectors must have an imaginary z-component. Assuming propagation along $\hat{y}$, consistently with the $\exp[+i(\mathbf{k}\cdot\mathbf{r} - \omega t)]$ representation, we look for modes with ω and k_y real. Therefore, the wavevectors read

$$\mathbf{k_1} = (0, k_y, i\beta_1), \tag{6}$$
$$\mathbf{k_2} = (0, k_y, -i\beta_2), \tag{7}$$

where the subscript "1" stands for the gyroelectric medium ($z > 0$), whereas "2" for the uniaxial medium ($z < 0$) and $Re[\beta_1],\ Re[\beta_2] > 0$. The main feature of our configuration is that TE and TM modes are not coupled, hence they obey the following dispersion relations

$$\begin{cases} k_y^2 - \beta_1^2 = \frac{\omega^2}{c^2}\epsilon_B, \\ k_y^2 - \beta_2^2 = \frac{\omega^2}{c^2}\epsilon_\perp, \end{cases} \tag{8}$$

$$\begin{cases} k_y^2 - \beta_1^2 = \frac{\omega^2}{c^2}\frac{\epsilon_g^2 - g^2}{\epsilon_g}, \\ \epsilon_{yy} k_y^2 - \epsilon_{zz}\beta_2^2 - 2ik_y\beta_2\epsilon_{yz} = \frac{\omega^2}{c^2}\epsilon_\parallel\epsilon_\perp, \end{cases} \tag{9}$$

where (8) hold for TE modes, whereas (9) rule the TM-modes propagation. As for TE modes, a simple calculation shows that the condition for evanescence $Re[\beta_1],\ Re[\beta_2] > 0$ is never satisfied for any value of the parameters, as for standard SPPs. Hence TE surface waves cannot propagate at the interface under consideration. Thus, our discussion will be focused on TM modes, characterized by the triplet (E_y, E_z, H_x). The magnetic field reads

$$\mathbf{H}_1 = (H_0, 0, 0)\ e^{ik_y y - \beta_1 z - i\omega t} \qquad z > 0, \tag{10}$$
$$\mathbf{H}_2 = (H_0, 0, 0)\ e^{ik_y y + \beta_2 z - i\omega t} \qquad z < 0. \tag{11}$$

We can evaluate the components of the electric field by means of Maxwell's equations:

$$\mathbf{E}_1 = \frac{H_0 e^{ik_y y+\beta_2 z-i\omega t}}{\omega\epsilon_0(\epsilon_g^2-g^2)}\,(0,\ -i\epsilon_g\beta_1 - igk_y,\ \epsilon_g k_y + g\beta_1), \tag{12}$$

$$\mathbf{E}_2 = \frac{H_0 e^{ik_y y+\beta_2 z-i\omega t}}{\omega\epsilon_0\epsilon_\parallel\epsilon_\perp}\,(0,\ i\epsilon_{zz}\beta_2-\epsilon_{yz}k_y,\ \epsilon_{yy}k_y-i\epsilon_{yz}\beta_2). \tag{13}$$

We can now evaluate the time-averaged Poynting vector as $\langle\mathbf{S}\rangle \equiv \frac{1}{2}\,\mathrm{Re}\,\{\mathbf{E}\times\mathbf{H}^*\}$. It turns out that

$$\langle\mathbf{S}_1\rangle = \frac{H_0^2 e^{-2Re\{\beta_1\}z}}{2\omega\epsilon_0(\epsilon_g^2-g^2)}\,Re\{(0,\ \epsilon_g k_y + g\beta_1,\ i\epsilon_g\beta_1 - igk_y)\}, \tag{14}$$

$$\langle\mathbf{S}_2\rangle = \frac{H_0^2 e^{2Re\{\beta_2\}z}}{2\omega\epsilon_0\epsilon_\parallel\epsilon_\perp}\,Re\{(0,\ \epsilon_{yy}k_y-i\epsilon_{yz}\beta_2,\ \epsilon_{yz}k_y-i\epsilon_{zz}\beta_2)\}. \tag{15}$$

By applying the continuity of E_y, we find the further condition

$$\epsilon_\parallel\epsilon_\perp(gk_y+\epsilon_g\beta_1) + (\epsilon_g^2-g^2)(i\epsilon_{yz}k_y+\epsilon_{zz}\beta_2) = 0, \tag{16}$$

which rules the propagation of the surface wave together with (9). These last two equations can be solved for β_1 and β_2, under the assumptions $\epsilon_g > g > 0$[22] and $\epsilon_\perp\epsilon_\parallel < 0$ as for HMs:

$$\beta_1 = \sqrt{k_y^2 - \epsilon_v\frac{\omega^2}{c^2}}, \tag{17}$$

$$\beta_2 = -i\frac{\epsilon_{yz}}{\epsilon_{zz}}k_y + \frac{1}{|\epsilon_{zz}|}\sqrt{\epsilon_\parallel\epsilon_\perp\left(k_y^2-\epsilon_{zz}\frac{\omega^2}{c^2}\right)}, \tag{18}$$

where we defined $\epsilon_v \equiv \frac{\epsilon_g^2-g^2}{\epsilon_g}$. Generally β_2 is a complex number, but evanescence is guaranteed in the anisotropic bulk, provided that $Re\,[\beta_2] > 0$. Keeping in mind that we are looking for solutions with both ω and k_y real, the only way for the SW to exist is considering β_2 as already divided in its real and imaginary parts, as written in (18). Thus, the quantity inside the square root must be positive. Hence

$$\epsilon_\parallel\epsilon_\perp\left(k_y^2-\epsilon_{zz}\frac{\omega^2}{c^2}\right) > 0 \qquad \overset{\epsilon_\perp\epsilon_\parallel<0}{\Longrightarrow} \qquad k_y^2 < \epsilon_{zz}\frac{\omega^2}{c^2}.$$

In addition, we should also require β_1 to be real and positive

$$\beta_1 > 0 \qquad \Longrightarrow \qquad k_y^2 > \epsilon_v\frac{\omega^2}{c^2}.$$

Combining the last two conditions yields $\epsilon_{zz} > \epsilon_v$, which implies $(\epsilon_\perp-\epsilon_\parallel)\cos^2\alpha > \epsilon_v - \epsilon_\parallel$. At this point there are two possible cases:

(a) $\epsilon_\perp > 0$, $\epsilon_\parallel < 0 \Longrightarrow \cos^2\alpha > \frac{\epsilon_v-\epsilon_\parallel}{\epsilon_\perp-\epsilon_\parallel}$. The condition $0 < \cos^2\alpha < 1$ yields to $\epsilon_\perp > \epsilon_v$.

(b) $\epsilon_\perp < 0$, $\epsilon_\parallel > 0 \Longrightarrow \cos^2\alpha < \frac{\epsilon_v-\epsilon_\parallel}{\epsilon_\perp-\epsilon_\parallel}$. The condition $0 < \cos^2\alpha < 1$ yields to $\epsilon_\parallel > \epsilon_v$.

Solving (16), (17) and (18) for k_y, we find

$$|k_y(\omega)| = \frac{\omega}{c}\sqrt{\frac{\epsilon_{zz}\left(\epsilon_g^2-g^2\right)^2 + \epsilon_g\left(\epsilon_\perp\epsilon_\parallel\right)^2 - \epsilon_\perp\epsilon_\parallel\left[\epsilon_g\left(\epsilon_g^2-g^2\right)+\epsilon_{zz}\left(\epsilon_g^2+g^2\right)\right] \pm \Delta}{\left(\epsilon_g^2-g^2\right)^2 + \left(\epsilon_\perp\epsilon_\parallel\right)^2 - 2\epsilon_\perp\epsilon_\parallel\left(\epsilon_g^2+g^2\right)}}, \tag{19}$$

where

$$\Delta = 2g\epsilon_g\left|\epsilon_\perp\epsilon_\parallel\right|\sqrt{\epsilon_{zz}^2 + \epsilon_\perp\epsilon_\parallel - \epsilon_{zz}\epsilon_g + \frac{\epsilon_{zz}}{\epsilon_g}\left(g^2-\epsilon_\perp\epsilon_\parallel\right)}.$$

Eq. (19) represents the dispersion relation of the surface wave[23]. It is to be remarked that the choice of the sign of $\pm\Delta$ in Eq.(19) corresponds to the choice of the sign of k_y, resulting in non-degenerate forward and backward propagating waves. In particular, $+\Delta$ corresponds to forward modes ($k_y > 0$), whereas $-\Delta$ corresponds to backward modes ($k_y < 0$). This is a typical non-reciprocal feature due to the presence of the magnetic field.

If both media do not exhibit dispersion, Eq. (19) reduces to a straight line on the $\omega - k$ plane. Instead, we assume that the HM has metal-like permittivities, i.e. we consider $\epsilon_\parallel = \epsilon_\perp\left(1-\frac{\omega_p^2}{\omega^2}\right)$, as for case (a)[24]. Three typical dispersion diagrams are shown in Fig. 2, wherein the red plot represents the case of non-gyrotropy. As we switch gyrotropy on, depending on the sign of the off-diagonal element g, the solution may assume a kink-behaviour, hence there are two distinct regimes characterized by different values of the group velocity.

The region of the plot we are interested in is for $\omega < \omega_p$ because the remaining part does not respect the assumption $\epsilon_\parallel\epsilon_\perp < 0$. In this regime, we notice that all plots end up in the same point on the $\omega = \omega_p$ line, regardless of the amount of gyrotropy affecting the system. This is due to the fact that $\epsilon_\parallel(\omega=\omega_p) = 0$. Such value of $\epsilon_\parallel$ lets Eq. (19) reduce to

$$|k_y(\omega=\omega_p)| = \frac{\omega_p}{c}\sqrt{\epsilon_{zz}(\omega=\omega_p)}, \tag{20}$$

which does not depend on g any more. For $\omega > \omega_p$, the existence conditions which let the surface wave have both ω and k_y real can no longer be satisfied.

III. ENERGY FLOW

The existence conditions let the time-averaged Pointing vector point towards $\hat{y}$, in particular

$$\langle \mathbf{S} \rangle = \begin{cases} \frac{H_0^2(\epsilon_g k_y + g\beta_1)}{2\omega\epsilon_0(\epsilon_g^2 - g^2)}\, e^{-2\beta_1 z}\, \hat{y} & z > 0, \\ \\ \frac{H_0^2 k_y}{2\epsilon_0 \epsilon_{zz}\omega}\, e^{2Re[\beta_2]z}\, \hat{y} & z < 0. \end{cases} \tag{21}$$

Thus, the flow of energy is correctly directed along the boundary, which guarantees an in-plane flow of energy. We notice that for $z > 0$ the energy flows towards $+\hat{y}$ for any value of the parameters, whereas in the lower half-space it can point towards $-\hat{y}$ if $\epsilon_{zz} < 0$. Overall, the total flux of energy is

$$\begin{aligned} \langle \mathcal{F} \rangle &= \int_{-\infty}^{\infty} \langle \mathbf{S} \rangle \, dz \\ &= \frac{H_0^2}{4\epsilon_0\omega} \left[\frac{g}{\epsilon_g \epsilon_v} + k_y \left(\frac{1}{\epsilon_v \beta_1} + \frac{1}{\epsilon_{zz} Re[\beta_2]} \right) \right] \hat{y}. \end{aligned} \tag{22}$$

Depending on the parameters we choose to consider, $\langle \mathcal{F} \rangle$ may be opposite to the direction of propagation[25]. In particular, this happens if

$$0 > \frac{1}{\epsilon_{zz}} > -\frac{Re[\beta_2]}{\epsilon_v} \left\{ \frac{1}{\beta_1} + \frac{g}{\epsilon_g k_y} \right\}. \tag{23}$$

Parameters that satisfy such inequalities allow the negative refraction of energy at the interface.

We can prove an important result related to the fields distribution in such systems. Let us focus our attention on the electric field lines in both upper and lower media. To do so, we have to consider the physical fields, represented by the real parts of (12)-(13), and then derive the equation of the field lines in the yz plane by means of

$$\frac{dz}{dy}(y,t) = \frac{Re[E_z(z,y,t)]}{Re[E_y(z,y,t)]}. \tag{24}$$

It turns out that the field lines in the gyroelectric medium are the same as the standard SPPs propagating between dielectric and metal. As for the HM, the field lines cannot be analytically evaluated if $\epsilon_{yz} \neq 0$, but the numerical results, obtained by solving Eq. (24) using Wolfram Mathematica, are shown in Fig. 3. We notice a tilted behaviour of the lines in the lower medium, which recalls the characteristic profile of the ZW [5, 6], even though we did not consider any lossy dielectric function. In addition, the tilted behaviour of the lines disappears when the off-diagonal element ϵ_{yz} is null, thus we can conclude that only anisotropy is responsible for this peculiar phenomenon. Adding some absorption would make the lines sink towards the interface, as for ZWs [5, 6].

The analytical results we derived in this section could be used to study less general situations by assigning proper values to the parameters, for instance if the upper medium is isotropic, in which case the solution is very similar to standard SPPs. In general, the surface waves we consider can be excited using the usual techniques, such as exploiting a coupling prism in a Otto configuration [3, 4], as shown below.

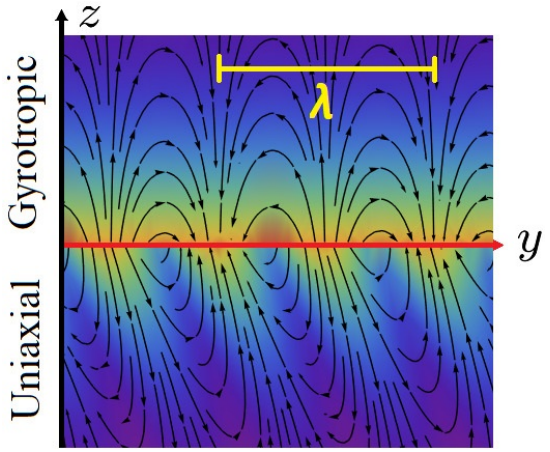

FIG. 3. Electric field lines of the TM mode that propagates at the interface between a gyroelectric and a hyperbolic medium. The parameters used are $\epsilon_g = 3$, $g = 1$, $\epsilon_\perp = 9$, $\omega = 4{\cdot}10^{14} Hz$ and $\omega_p = 5 \cdot 10^{14} Hz$ (corresponding to $\epsilon_\parallel \approx -5.06$). The obtained in-plane wavelength is $\lambda = \frac{2\pi}{k_y} = 2.79\ \mu m$, which is shown in the figure as a comparison length. The penetration depths are $l_p^{gyro} = \frac{1}{\beta_1} \approx 1.8\ \mu m$ and $l_p^{uni} = \frac{1}{Re[\beta_2]} \approx 0.4\ \mu m$, respectively.

IV. InSb-GRAPHENE AHMM INTERFACE AT MID-INFRARED FREQUENCIES

It is not so easy to find a proper material which shows a gyroelectric behaviour at reasonable temperatures and frequencies. The most famous examples of gyroelectric media are cold plasmas subjected to an external homogeneous magnetic field. However, when it comes to practical uses, plasmas are difficult to confine and it is not trivial to deal with their temperatures. On the other hand, some semiconductors have been proven to have a gyroelectric response at some particular frequencies when a magnetic bias is switched on. For example, Indium Antimonide (InSb) dielectric response can be modeled as [26, 27]

$$\epsilon_g = \epsilon_0 \epsilon_\infty \left(1 - \frac{\omega_p^2 \left(\omega^2 + i\gamma\omega\right)}{\left(\omega^2 + i\gamma\omega\right)^2 - \omega_c^2 \omega^2} \right), \tag{25}$$

$$g = \epsilon_0 \epsilon_\infty \frac{i\omega_p^2 \omega_c \omega}{\left(\omega^2 + i\gamma\omega\right)^2 - \omega_c^2 \omega^2}, \tag{26}$$

$$\omega_p = \sqrt{\frac{Ne^2}{\epsilon_0 \epsilon_\infty m^*}}, \quad \omega_c = \frac{eB}{m^*}, \tag{27}$$

where ω_p is the plasma frequency, ω_c is the cyclotron frequency, γ is the damping coefficient, N is the electron

density, m^* is the effective mass and B is the external magnetic bias. In our case, one can properly choose both the electron density and the external magnetic field such that the existence conditions are satisfied.

As for the hyperbolic medium, many artificial structures have been shown to generate hyperbolic anisotropy. The most remarkable ones are a stack of alternating metallic and dielectric layers (Multilayer) and a lattice of metallic nanowires embedded in a dielectric background (Nanowire Array). Such engineered media are known as Hyperbolic Metamaterials (HMMs) [28, 29]. Aiming for a multilayer structure, let us consider a material composed of a succession of metallic and dielectric layers, whose thicknesses and dielectric constants are, respectively, l_d, ϵ_d and l_m, ϵ_m. If the growth direction is $\hat{y}$, by means of an effective medium approximation it can be shown that the overall dielectric tensor of such composite material has the form (2), with

$$\epsilon_\perp = \frac{l_d\epsilon_d + l_m\epsilon_m}{l_d + l_m} = (1-f)\epsilon_d + f\epsilon_m, \tag{28}$$

$$\epsilon_\parallel = \frac{l_d + l_m}{l_d\epsilon_d^{-1} + l_m\epsilon_m^{-1}} = \frac{1}{(1-f)\epsilon_d^{-1} + f\epsilon_m^{-1}}, \tag{29}$$

where f is the *fill fraction* and it is defined as $f \equiv \frac{l_m}{l_m+l_d}$ [28, 29]. If the growth direction does not lie on the interface plane, the HMM is referred to as *Asymmetric Hyperbolic Metamaterials* (AHMMs) and its physical configuration is depicted in Fig. 1.

Graphene layers stuck in a host matrix can exhibit a hyperbolic behaviour [30]; their dielectric response can be modeled as

$$\epsilon_\parallel = \epsilon_h, \tag{30}$$

$$\epsilon_\perp = \epsilon_h + i\frac{\sigma(\omega)}{d\omega\epsilon_0}, \tag{31}$$

where ϵ_h is the dielectric constant of a host matrix, d is the distance between the two-dimensional graphene layers and $\sigma(\omega)$ is the surface conductivity [31, 32]. If the optical axis is tilted with respect to the interface, we have a graphene-based AHMM [31, 33]. One can properly choose the host matrix and the periodicity d in order to minimise the losses due to the imaginary part of $\epsilon_\perp$, as Nefedov and Melnikov showed in [33], and satisfy the existence conditions of the surface wave.

In order to show how the SW here predicted could be observed in such a system, we have studied the reflection properties of a InSb-Graphene AHMM interface in the Otto configuration, where Thallium Bromo-Iodide (KRS5) was used as the coupling medium. Fig. 4(a) shows the reflectivity of the system as a function of the light frequency and the incidence angle θ, calculated using the 4×4 Transfer Matrix Formalism for anisotropic media, proposed by Berreman [34]. For each value of the frequency, we notice that the reflectivity significantly drops near a certain value of the incidence angle θ. For that particular value of θ, the in-plane component of the wavevector gives rise to the coupling between bulk and surface modes. In addition, here we can easily observe the non-reciprocal behaviour of these SWs, as the spectra shown in Fig. 4 are not symmetric with respect to $\theta = 0$. Six different sections of the reflectivity plot are shown in Fig. 4(b), where the effects of the excitation of the SW can be observed more clearly. As an example to quantify the effect of losses (here essentially due to those in the gyroelectric medium), the propagation length of the forward propagating mode at $\omega = 1100\ cm^{-1}$, defined as $l_p \equiv \frac{1}{2Im[k_y]}$, amounts to $l_p \approx 40\lambda$. We can conclude that InSb and a graphene-based AHMM could be exploited in order to excite and detect the novel modes here predicted.

V. CONCLUSIONS

The propagation of a novel type of electromagnetic surface wave at the interface between a hyperbolic medium and a gyroelectric material was discussed by both theoretical analysis and electromagnetic simulations. The theoretical results showed that gyrotropy is responsible for the non reciprocal multiplicity of these TM-polarized modes, whereas the anisotropy of the lossless hyperbolic medium is responsible for a tilted behaviour in the field lines, which resemble those of the Zenneck Waves for lossy metals. Frequency dispersion of the response functions has also been taken into account. Finally, a physical system which is suitable to support the propagation of the surface waves here predicted has been proposed: by exploiting the properties of doped InSb in a magnetic field and a graphene-based asymmetric hyperbolic metamaterial, it could be possible to excite and detect such modes in a Otto configuration.

[1] J. Zenneck, Über die fortpflanzung ebener elektromagnetischer wellen längs einer ebenen leiterfläche und ihre beziehung zur drahtlosen telegraphie, Annalen der Physik **328**, 846 (1907).

[2] J. A. Polo and A. Lakhtakia, Surface electromagnetic waves: A review, Laser & Photonics Reviews **5**, 234 (2011).

[3] S. Maier, Plasmonics: Fundamentals and applications (2007) p. 245.

[4] A. Zayats, I. Smolyaninov, and A. Maradudin, Nano-optics of surface plasmon polaritons, Physics Reports001 132 A.V. Zayats et al. Physics Reports **4082011**, 131 (2005).

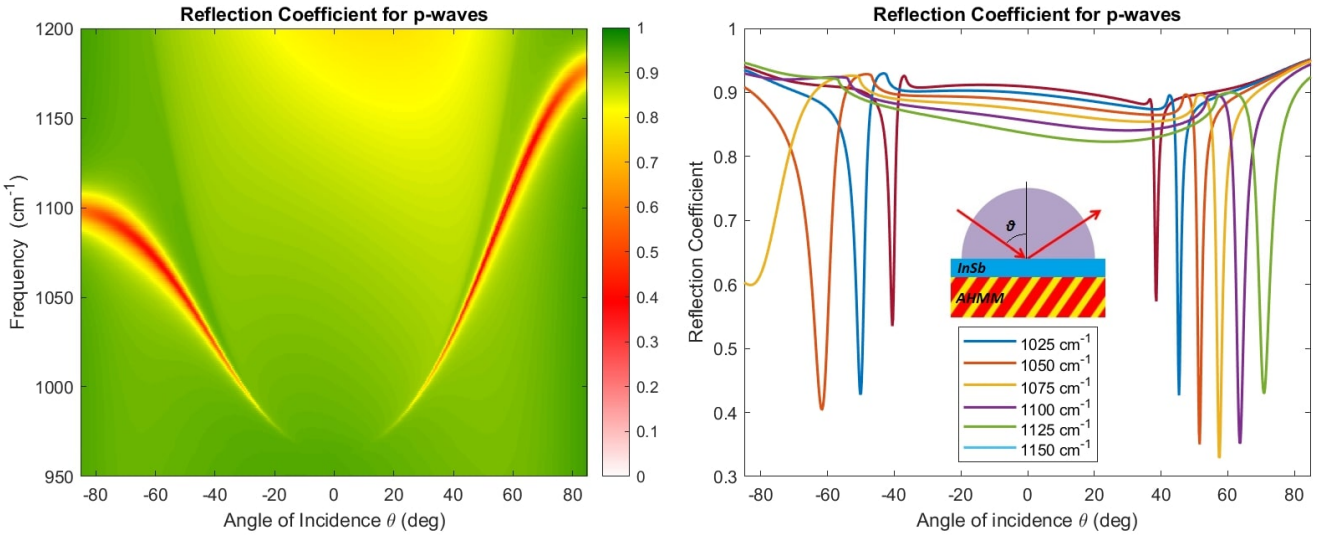

FIG. 4. (a) Numerical results for the reflectivity of the Otto configuration with $d_{InSb} = 1.1\ \mu m$ and $\alpha = \frac{\pi}{4}$. (b) Reflectivity as a function of the incidence angle, for different values of the frequency.

[5] S. Oruganti, F. Liu, D. Paul, J. Liu, J. Malik, K. Feng, H. Kim, Y. Liang, T. Thundat, and F. Bien, Experimental realization of zenneck type wave-based non-radiative, non-coupled wireless power transmission, Scientific Reports **10**, 925 (2020).

[6] F. Jangal, N. Bourey, M. Darces, F. Issac, and M. Hélier, Observation of zenneck-like waves over a metasurface designed for launching hf radar surface wave, International Journal of Antennas and Propagation **2016**, 1 (2016).

[7] M. Dyakonov, New type of electromagnetic wave propagating at an interface, Journal of Experimental and Theoretical Physics **94**, 119 (1988).

[8] H. Huang, Y. Fan, B.-I. Wu, F. Kong, and J. Kong, Surface modes at the interfaces between isotropic media and uniaxial plasma, Progress In Electromagnetics Research **76** (2007).

[9] Z. Jacob and E. E. Narimanov, Optical hyperspace for plasmons: Dyakonov states in metamaterials, Applied Physics Letters **93**, 221109 (2008).

[10] R. Camley, Nonreciprocal surface waves, Surface Science Reports **7**, 103 (1987).

[11] F. Alexander and L. Barkovsky, A new type of surface polaritons at the interface of the magnetic gyrotropic media, Journal of Physics A: Mathematical and Theoretical **40**, 309 (2006).

[12] F. Alexander and L. Barkovsky, Surface polaritons at the planar interface of twinned dielectric gyrotropic media, Electromagnetics **28**, 146 (2008).

[13] D. Ignatyeva, A. Kalish, G. Levkina, and A. Sukhorukov, Surface plasmon polaritons at gyrotropic interfaces, Phys. Rev. A **85** (2012).

[14] A. Boardman, N. King, Y. Rapoport, and L. Velasco, Gyrotropic impact upon negatively refracting surfaces, New Journal of Physics **7** (2005).

[15] A. Moradi and M. Wubs, Strongly direction-dependent magnetoplasmons in mixed faraday–voigt configurations, Scientific Reports **11**, 18373 (2021).

[16] O. Takayama, A. A. Bogdanov, and A. V. Lavrinenko, Photonic surface waves on metamaterial interfaces, Journal of Physics: Condensed Matter **29**, 463001 (2017).

[17] J. Polo, T. Mackay, and A. Lakhtakia, Electromagnetic surface waves: A modern perspective (2013) pp. 1–293.

[18] J. A. Polo, S. Nelatury, and A. Lakhtakia, Surface waves at a biaxial bicrystalline interface, Journal of the Optical Society of America A **24**, 2974 (2007).

[19] A. Lakhtakia, T. Mackay, and C. Zhou, Electromagnetic surface waves at exceptional points, European Journal of Physics **42** (2020).

[20] C. Zhou, T. Mackay, and A. Lakhtakia, Two dyakonov–voigt surface waves guided by a biaxial–isotropic dielectric interface, Scientific Reports **10**, 12894 (2020).

[21] E. Cojocaru, Dyakonov hybrid surface waves at the isotropic-biaxial media interface, J. Opt. Soc. Am. A **32**, 782 (2015).

[22] The condition $g < \epsilon_g$ guarantees modes propagation in the gyroelectric medium.

[23] In the particular case where $g = 0$ and $\epsilon_\perp = \epsilon_\parallel < 0$, Eq. (19) reduces to the dispersion relation of the SPP propagating through a metal-dielectric interface.

[24] Case (b) shows similar features, hence it will not be investigated in detail here.

[25] This result has already been shown for particular interfaces, including left-handed media [8].

[26] E. Moncada-Villa, A. Fernández-Domínguez, and J. Cuevas, Magnetic-field controlled anomalous refraction in doped semiconductors, Journal of the Optical Society of America B **36**, 935 (2019).

[27] J. Chochol, K. Postava, M. Cada, M. Vanwolleghem, L. Halagačka, D. Vignaud, J.-F. Lampin, and J. Pištora, Magneto-optical properties of insb for terahertz applications, AIP Advances **6** (2016).

[28] L. Ferrari, C. Wu, D. Lepage, X. Zhang, and Z. Liu, Hyperbolic metamaterials and their applications, Progress in Quantum Electronics **40** (2014).

[29] P. Shekhar, J. Atkinson, and Z. Jacob, Hyperbolic metamaterials: Fundamentals and applications, Nano Convergence **1** (2014).

[30] I. Iorsh, I. Mukhin, I. Shadrivov, P. Belov, and Y. Kivshar, Hyperbolic metamaterials based on multilayer graphene structures, Physical Review B **87** (2012).
[31] I. Nefedov, C. Valagiannopoulos, S. M. Hashemi, and E. Nefedov, Total absorption in asymmetric hyperbolic media, Scientific reports **3**, 2662 (2013).
[32] A. Dubinov, V. Aleshkin, V. Mitin, T. Otsuji, and V. Ryzhii, Terahertz surface plasmons in optically pumped graphene structures, Journal of physics: Condensed matter **23**, 145302 (2011).
[33] I. Nefedov and L. Melnikov, Plasmonic terahertz amplification in graphene-based asymmetric hyperbolic metamaterial, Photonics **2**, 594 (2015).
[34] D. Berreman, Optics in stratified and anisotropic media: 4×4 matrix formulation, Journal of The Optical Society of America **62** (1972).